Supercritical Brayton Power Conversion with a Direct Cooled Reactor for Space Power

Becky Sondelski, Alex Swenson, Greg Nellis, Mark Anderson, Paul Wilson
University of Wisconsin – Madison

AUTHOR BIOGRAPHIES

Becky Sondelski – Mechanical Engineering
Becky is a Master of Science degree candidate in Mechanical Engineering at UW-Madison. She graduated with a Bachelor's degree in Mechanical Engineering from the Milwaukee School of Engineering in 2017. Her research focuses on modeling mass optimization for a Brayton Cycle space power plant, and her other research interests include thermal sciences and the aerospace industry.

Alex Swenson – Nuclear Engineering, Engineering Physics
Alex is a Master of Science candidate in Nuclear Engineering and Engineering Physics at UW-Madison. He graduated with a Bachelor's degree in Nuclear Engineering from UW-Madison in 2017. His research interests are reactor physics and computational nuclear analysis.

Greg Nellis – Mechanical Engineering
Greg Nellis is a Professor of Mechanical Engineering. Dr. Nellis has experience studying thermal-fluid systems including cryogenic and room temperature refrigeration cycles and supercritical CO2 systems.

Paul Wilson – Engineering Physics
Paul Wilson is the Grainger Professor of Nuclear Engineering in the University of Wisconsin-Madison's Department of Engineering Physics. His research interests focus on developing improved tools for computational modeling of complex nuclear energy systems, with applications in radiation shielding, nuclear waste management, nuclear non-proliferation and energy policy.

Mark Anderson – Mechanical Engineering
Dr. Mark Anderson is a professor in the Department Mechanical Engineering and Director of the University of Wisconsin's Thermal Hydraulic Laboratory. Dr. Anderson studies both the physics, thermal hydraulic performance related to sCO2 Brayton cycles.

ABSTRACT

To achieve future goals in space exploration a long life, compact power system will be necessary, and nuclear power sources are a promising option. The goal of this project is to achieve mass optimization with a supercritical Brayton Cycle coupled to a direct-cooled nuclear reactor. It is critical to minimize the total mass of this system because of space launch costs. The total mass involves both the components' masses as well as the fuel mass which is related to system efficiency. This paper discusses a project in which a detailed reactor model is integrated with a carefully constructed cycle model in order to simultaneously optimize the design of these two aspects of the system. Component models are discussed as well as an initial optimization study. A robust, simple recuperated Brayton cycle model is complete and is in the process of integration with a developing reactor model. Preliminary observations of the cycle model have led to the conclusion that there will be an optimum point between a large recuperator and small reactor with high system efficiency, and a large reactor and small recuperator with low recuperator mass for any given radiater size. Once the reactor model is integrated into the cycle optimization, the tradeoffs between the sizes of the radiator, recuperator, and reactor will be

further investigated and an optimum system mass will be apparent.

INTRODUCTION

A model with optimization capabilities was created for the Brayton cycle shown in Figure 1 to allow minimization of the system mass. To enable studies that span a range of conditions, cycle configurations, and fluids, models for each cycle component were constructed separately and carefully, ensuring that they were robust and accurate as well as computationally efficient. The component models were then integrated to allow cycle simulation. The cycle model is integrated with an optimization algorithm to allow comprehensive design studies.

The reactor design is being developed in conjunction with the system power cycle rather than in isolation from it so that these two parts of the system can be optimized simultaneously. This approach differs from traditional nuclear power plant design, because the total system mass is intrinsically coupled by flow conditions, cycle efficiency and desired electrical output. The reactor design will be distinct from terrestrial designs in the parameters optimized. Terrestrial reactors are designed to produce large amounts of electricity for low cost; this design will focus on limiting mass. The reactor design process will be integrated as a part of a holistic system optimization, rather than separately designing a power cycle that is compatible with a fixed reactor design. To this end, a surrogate reactor physics model will be developed for direct integration into the system model, allowing reactor parameters to be modified by the optimization process. Such a surrogate model will be generated by parametric analysis using standard high-fidelity (but computationally slow) reactor physics tools.
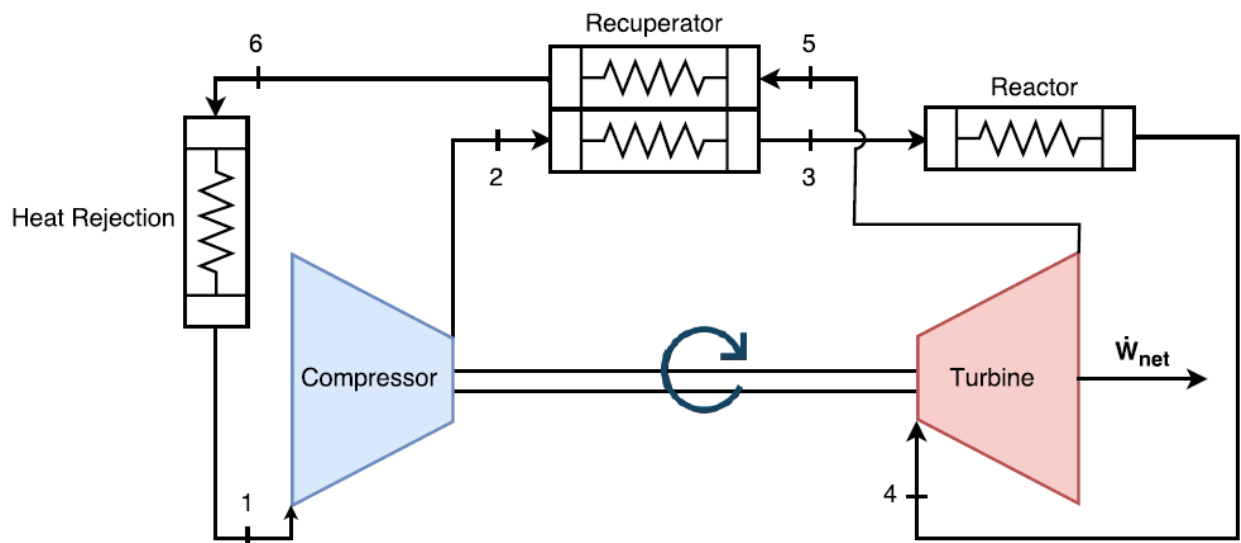

Figure 1: Simple, recuperated Brayton cycle

POWER CYCLE

Heat Exchanger Component Model

The recuperator is modeled as being in a counter-flow configuration using a sub-heat exchanger technique that employs the effectiveness-NTU method. This method allows the user to set the conductance of the heat exchanger as a performance metric and, based on this conductance, computes the performance under specific cycle conditions. This technique works well because, for a particular geometry, the conductance of a heat exchanger is an accurate predictor of its mass. The model allows the outlet temperatures to be calculated when each sides' inlet temperature, mass flow rate, and

pressure are known along with the overall conductance.

The heat exchanger was discretized into sub-heat exchangers, as depicted in Figure 2, to account for the changes in the working fluid properties that occur in the supercritical region of CO2. The enthalpy of the fluid was found using one of two different fluid databases. The first fluid database used was NIST's Reference Fluid Thermodynamic and Transport Properties Database (REFPROP) [1]. REFPROP is comprehensive in the fluid options that can be used and the temperature and pressure ranges that are covered; however, it is computationally expensive. The second fluid database used was the Fluid Interpolation Tables (FIT), a Toolbox Add-On for MATLAB [2]. FIT is currently limited to supercritical CO_2 with a limited temperature and pressure range; however, FIT is very computationally efficient.
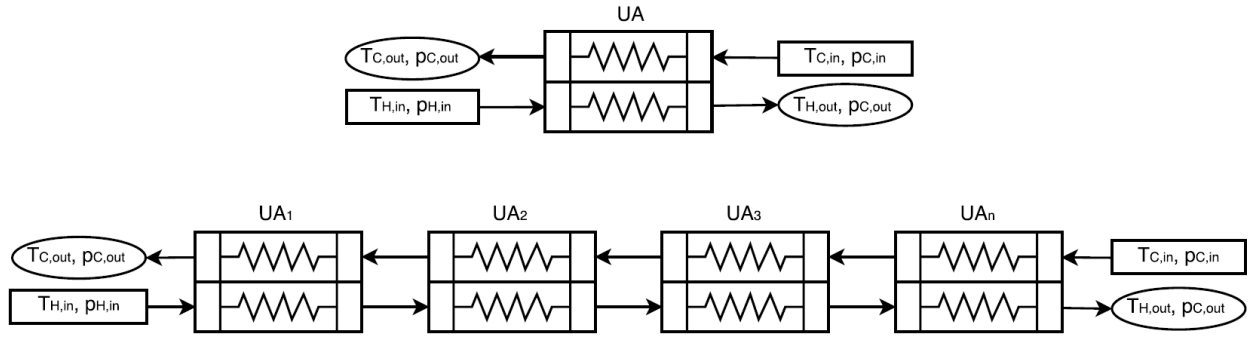

Figure 2: Visual representation of sub-heat exchanger breakdown

For both the overall heat exchanger and the sub-heat exchangers, an energy balance leads to the general result that the heat transfer rate is associated with a change in the enthalpy of the fluid:

$$\dot{Q} = \dot{m}\Delta h \tag{1}$$

With given inlet conditions for the overall heat exchanger and a guessed value for the hot side outlet temperature (and therefore enthalpy), Equation (1) can be used to calculate the rate of heat transfer and the cold side outlet enthalpy (and temperature).

The heat exchanger is discretized such that the rate of heat transfer is the same for each sub-heat exchanger. Since the inlet temperatures of the first sub-heat exchanger are known, the corresponding enthalpies, and the heat transfer are known, and the outlet condition can be determined. In general, the exit enthalpy for each sub-heat exchanger can be found using an energy balance:

$$h_{i+1} = h_i - \frac{\dot{Q}}{N\dot{m}} \tag{2}$$

The Effectiveness-NTU method is used to find the conductance of all the sub-heat exchangers [3, 4]. For this method, it is necessary to find the capacitance rate ($\dot{C}$) for both streams in each sub-heat exchanger using the equation:

$$\dot{C} = \dot{m}\left(\frac{h_{in} - h_{out}}{T_{in} - T_{out}}\right) \tag{3}$$

Using the lower of the two capacitance rates, the ratio of the actual heat transfer rate to the maximum possible heat transfer rate, otherwise known as the effectiveness (ε), of each sub-heat exchanger can be found as follows:

$$\varepsilon = \frac{\dot{Q}}{N\dot{C}_{min}\left(T_{H,in} - T_{C,in}\right)} \tag{4}$$

The capacity ratio (C_R) is found as the ratio of the smaller capacitance rate to the larger capacitance rate:

$$C_R = \frac{\dot{C}_{min}}{\dot{C}_{max}} \tag{5}$$

The effectiveness and capacity ratio can be used to find the number of transfer units (NTU):

$$NTU = \begin{cases} \dfrac{\ln\left[\dfrac{1 - \varepsilon C_R}{1 - \varepsilon}\right]}{1 - C_R} & \text{for } C_R < 1 \\[4mm] \dfrac{\varepsilon}{1 - \varepsilon} & \text{for } C_R = 1 \end{cases} \tag{6}$$

The NTU and the minimum capacitance rate can then be used to find the conductance for each sub-heat exchanger:

$$UA_i = NTU\,\dot{C}_{min} \tag{7}$$

Finally, the conductance from each sub-heat exchanger can be summed to find the conductance of the overall heat exchanger:

$$UA = \sum_{i=1}^{N} UA_i \tag{8}$$

This conductance value, calculated using a guessed outlet temperature, is then compared to the given conductance value for the overall heat exchanger (an input to the model). This comparison provides an error value.

The first step in solving for the actual hot side outlet temperatures is to find error values for several initial guesses for the hot side outlet temperature. The range of the initial guesses is defined by the inlet temperatures of the hot and cold sides. If the guessed temperature for the hot side outlet is too close to the cold side inlet, then the result may not be physical (i.e., the temperature streams would have to cross and the effectiveness of some sub-heat exchanger would become greater than 1 or less than 0). The resulting error value is meaningless because using the effectiveness-NTU relation results in a calculated conductance that is a complex number; this result must be discarded during the iteration process. However, as the guessed temperature approaches the hot side inlet temperature, the error values become decreasingly positive real numbers until they cross zero and become increasingly negative real numbers. The result of this analysis provides a temperature range where the error values are all real and range from a negative value to a positive value. This acceptable temperature range is subsequently provided along with the error function itself as the plant for the MATLAB fzero function which is a sophisticated root finding technique that can accurately and quickly find the unique hot side outlet temperature that produces the input conductance.

The effect of the number of sub-heat exchangers was analyzed to find the appropriate balance between accuracy (with more sub-heat exchangers) and speed (with fewer). Table 1 shows the parameters that

were input into the model for this analysis. Three separate sets of parameters were selected to test the consistency of results across different conditions. All the selected sets of operating conditions forced the model through the pseudocritical point in order to provide the most rigorous test.

Table 1: Parameters for studying number of sub-heat exchangers and the termination tolerance

	Hot Side			Cold Side				
	Inlet Temperature [K]	Pressure [kPa]	Mass Flow Rate [kg/s]	Inlet Temperature [K]	Pressure [kPa]	Mass Flow Rate [kg/s]	Conductance [W/K]	Fluid
1	900	7390	1.5	290	7390	1.5	1210	CO2
2	600	7390	1.5	290	7390	0.5	1210	CO2
3	800	4800	1.5	400	4800	0.5	1210	Acetone

For the various operating conditions, the outlet temperatures were observed over a range of 1-100 sub-heat exchangers. The error in outlet temperatures of each test run were defined assuming that the outlet temperature calculated with 100 sub-heat exchangers is the correct value. These results are shown in Figure 3.
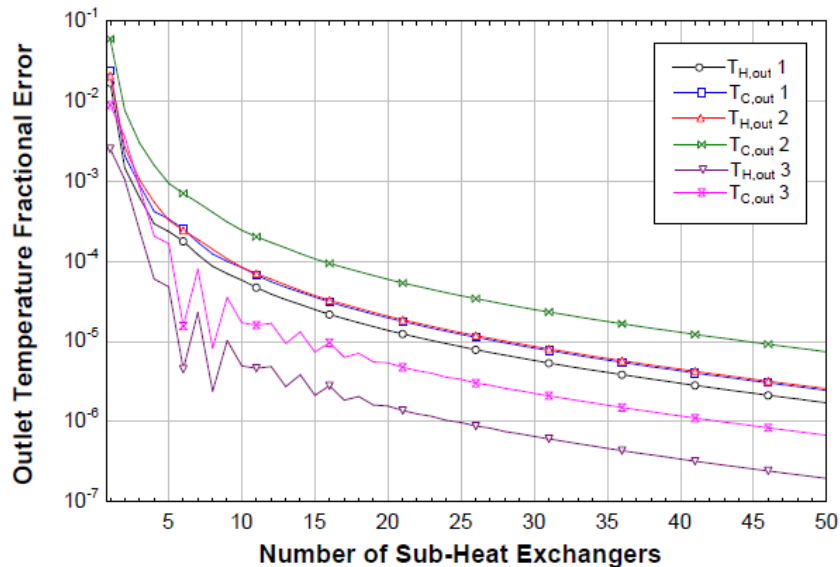

Figure 3: Accuracy of outlet temperature results as a function of the number of sub-heat exchangers

It appears that the outlet temperature converges using approximately 10 sub-heat exchangers. To be more precise, the outlet temperatures had converged to within three decimal places when 20 sub-heat exchangers are used and to within two decimal places when 10 sub-heat exchangers were used. As a result, 20 sub-heat exchangers were used for the model.

Turbomachinery on-Design Behavior

The design point efficiency of a turbomachine can be correlated against specific speed and specific diameter making use of the similarity concept. The specific speed (n_s) describes the rotor speed of an ideal, geometrically similar impeller sized to deliver one unit of volume over one unit of time against one

unit of isentropic enthalpy change. For compressors and turbines, the specific speed is defined as:

$$n_s = \frac{\omega \sqrt{\dot{V}}}{\Delta h_s^{\frac{3}{4}}}$$

(9)

Here, ω represents the angular velocity (in radians per second) and $\dot{V}$ is the volumetric flow rate. The volumetric flow rate remains constant for incompressible media, but when the fluid is compressible, the inlet and outlet flows are not equal. For turbines, it is common practice to use the exit flow rate whereas for compressors, the inlet flow rate is used. Δh_s represents the enthalpy change that would occur if the turbomachine was isentropically compressing the fluid to the same exit pressure.

In the same way, the specific diameter (d_s) is the rotor diameter (D) of an ideal, geometrically similar impeller sized to deliver one unit of volume over one unit of time against one unit of head change. The specific diameter is defined as:

$$d_s = \frac{D \Delta h_s^{\frac{1}{4}}}{\sqrt{\dot{V}}}$$

(10)

Design point efficiency as a function of specific speed and specific diameter has been compiled by O. E. Balje for compressors and turbines and used to generate contour plots [5]. The contour plot for compressor efficiency as a function of specific speed and specific diameter can be seen in Figure 4.
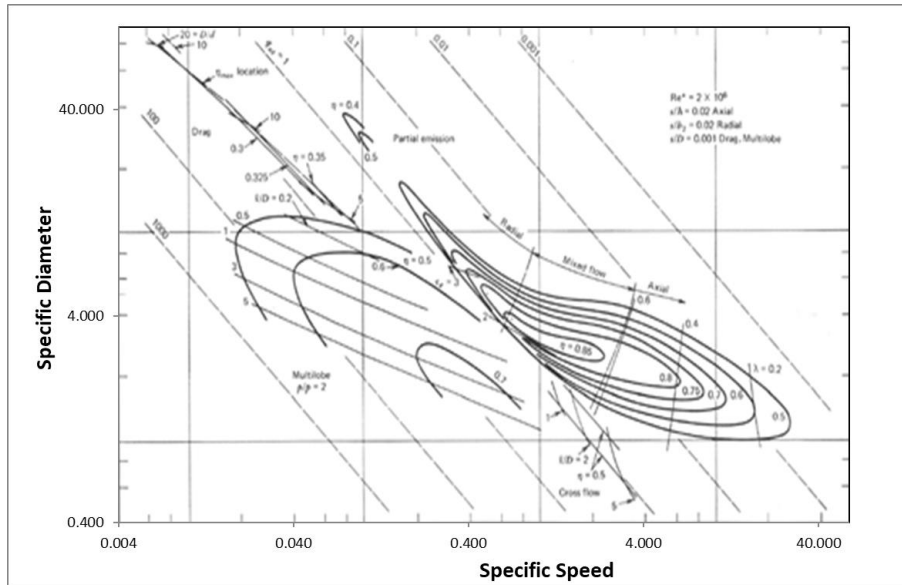

Figure 4: $n_s d_s$ diagram for single stage compressors (from [5]).

A computationally efficient and robust method is required to estimate the design point efficiency given specific speed and specific diameter values in order to provide the required turbomachinery component models. Therefore, an equation-based representation of the three-dimensional surface is desirable. The formula for the curve fit of efficiency as a function of specific diameter and specific speed is defined as:

$$\eta(d_s, n_s) = \eta_{max}(n_s) \exp\left[-\frac{\left(\log_{10} d_s - \log_{10} d_{s,c}(n_s)\right)^2}{\sigma_{ds}(n_s)^2}\right] \tag{11}$$

Note that at a given value of specific speed (i.e., along a vertical line in Figure 4) the efficiency approximately fits a Gaussian function of the log (base 10) of the specific diameter. The parameters that are used to describe the curve fit at each specific speed are η_{max}, the maximum efficiency for the specific speed studied, $\log_{10} d_{s,c}$, the logarithm of the specific diameter corresponding to the maximum efficiency which represents the center of the Gaussian curve, and σ_{ds}, a term related to the width of the curve. This fitting process was repeated several times at various specific speeds which resulted in several values of each of the parameters, η_{max}, $\log_{10} d_{s,c}$, and σ_{ds}. These values were subsequently fit to functions of specific speed.

A high order polynomial was used to fit the parameter relating to the curve center, $\log_{10} d_{s,c}$, as a function of the specific speed. The polynomial was manually adjusted to better fit the higher efficiency contours. The final result is shown in Figure 5.
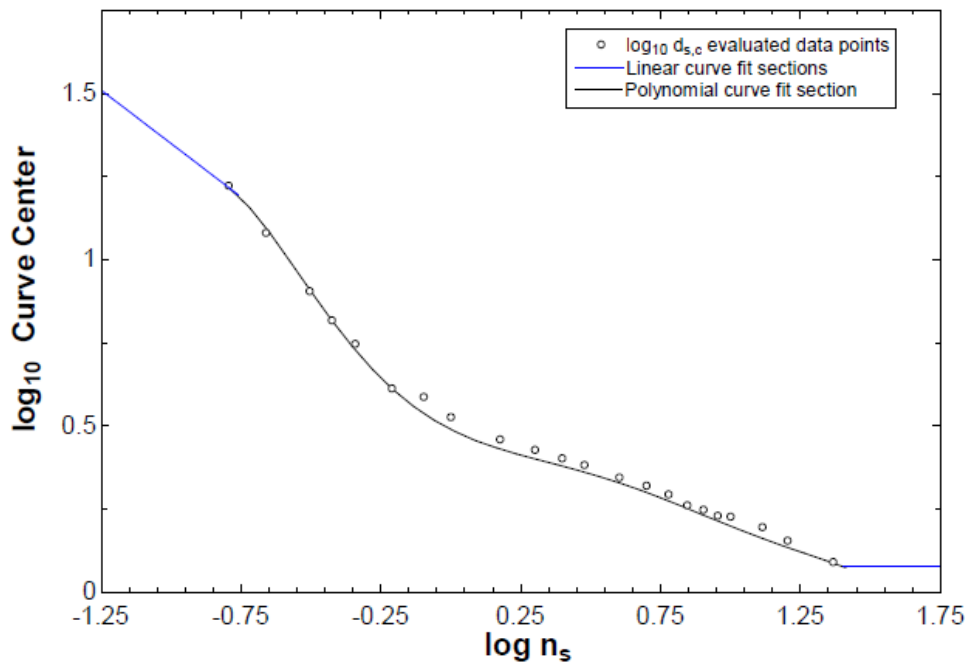

Figure 5: EES polynomial fit for term corresponding to the curve's center – manually adjusted

To avoid unrealistic results outside of the data range, a piecewise function was created for the regions above and below the polynomial fit. A line tangent to the end of the polynomial at the first data point and a line horizontal from the last data point were used outside of the data range, leading to the function:

$$
\log_{10} d_{s,c}(n_s) = \begin{cases} -0.6433x + 0.7068 & , \quad x < -0.79 \\[2mm] \begin{aligned} 0.4890 - 0.4264x + 0.6387x^2 - 0.6370x^3 \\ - 0.2498x^4 + 0.5800x^5 - 0.1965x^6 \end{aligned} & , \quad -0.79 < x < 1.4 \\[2mm] 0.0764 & , \quad x > 1.4 \end{cases} \qquad (12)
$$

Here, the term x is $\log_{10}(n_s)$.

In the same way, a high order polynomial fit was found for the maximum efficiency term. Here, to be sure the range outside the data points was realistic, exponential functions were fit to each end of the curve causing the efficiency to smoothly decay to zero outside of the contours. Again, the polynomial was manually adjusted to better fit the higher efficiency contours. The resulting function can be found in Figure 6.
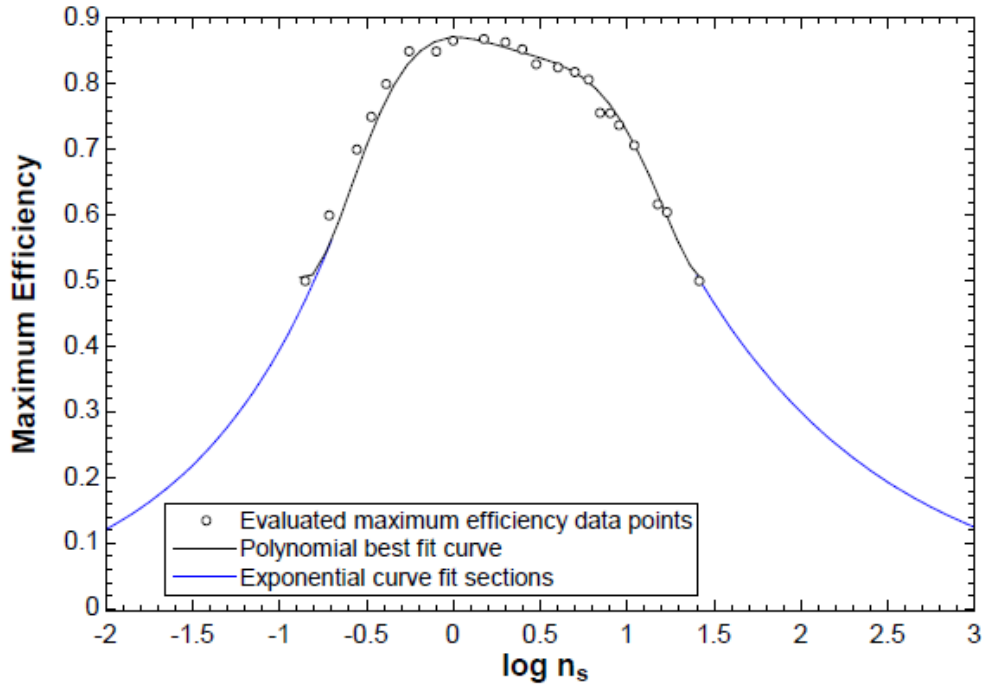

Figure 6: Polynomial fit for term corresponding to the compressor maximum efficiency – manually adjusted

The equation for this function is found as:

$$
\eta_{max}(n_s) = \begin{cases} 1.289(3.265)^x & , \quad x < -0.68 \\[2mm] \begin{aligned} 0.8709 + 0.0146x - 0.3817x^2 + 0.6176x^3 \\ - 0.1331x^4 - 0.5645x^5 + 0.2843x^6 \end{aligned} & , \quad -0.68 < x < 1.4 \\[2mm] 1.745(0.4144)^x & , \quad x > 1.4 \end{cases} \qquad (13)
$$

Here, the term x is $\log_{10}(n_s)$.

For the curve width term, a polynomial was used as shown in Figure 7. Outside the range of useful data

points, this term is modeled as a constant. At very large specific speed values, the curve width term is a value near the highest data point. At very small specific speed values, the curve width term is a value near the lowest data point.
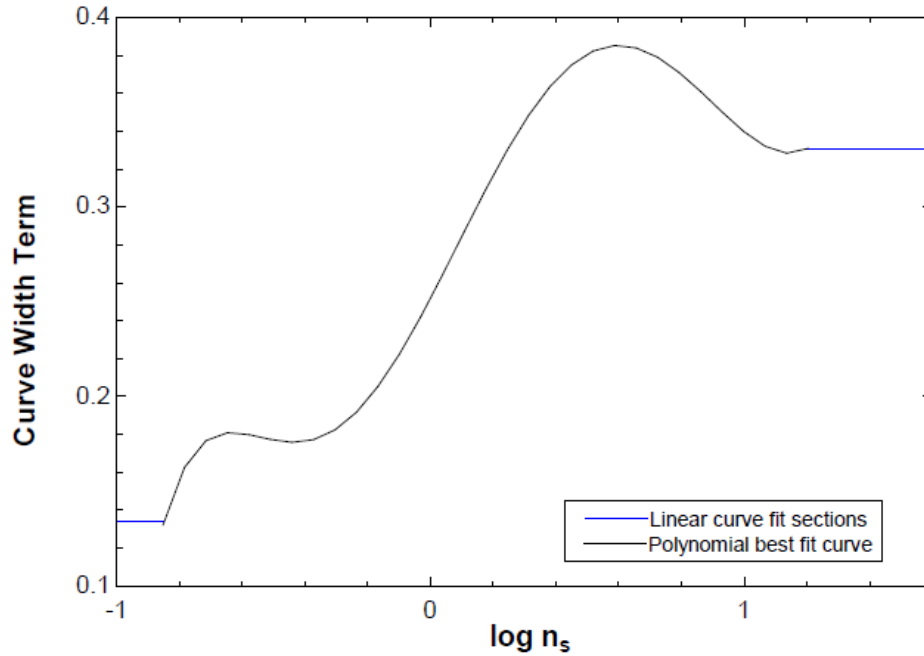

Figure 7: Polynomial fit for term corresponding to the compressor curve's width

The equation for this function is found as:

$$\sigma_{ds}(n_s) = \begin{cases} 0.1341 & , & x < -0.85 \\ \begin{aligned} 0.2516 + 0.3178x + 0.1485x^2 - 0.5626x^3 \\ - 0.1301x^4 + 0.4288x^5 - 0.1143x^6 \end{aligned} & , & -0.85 < x < 1.2 \\ 0.3306 & , & x > 1.2 \end{cases} \tag{14}$$

Here, the term x is $\log_{10}(n_s)$.

A MATLAB function was created that takes an input of specific speed and specific diameter and returns the corresponding efficiency. First, the specific speed is used to find the parameters for the Gaussian curve, the maximum efficiency, the curve's center value, and the term corresponding to the curve's width. Then the specific diameter is input into the resulting Gaussian curve and an efficiency is found. The function is much faster than other currently available methods, such as bilinear interpolation. In addition, Eqs. (12) and (13), together, provide the relationship between specific speed and specific diameter that defines the peak of the contours and the associated efficiency at that peak. For on-design simulations it is useful to constrain the turbomachine to remain on this optimal operating line.

The function developed using this technique yields the efficiency contour plot shown in Figure 8. The contour plot created is shown as an overlay over the actual Balje curves.
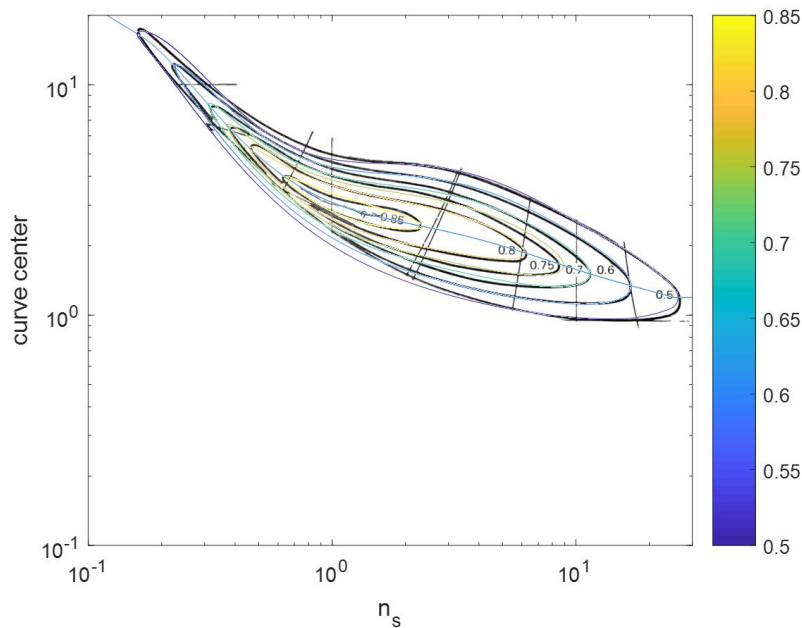
Figure 8: Function efficiency contour plot overlay on actual Balje plot

To test the accuracy of the function, several specific speed and specific diameter values were selected and used to find compressor efficiency using both the created function and the data digitally obtained from the Balje curve. 98% of the efficiency values obtained from the function were within 20% error from the digitized data and 70% of the efficiency values were within 10% error. However, it was observed that the digitized data created superficial local maxima which compromised the accuracy of the efficiency solutions from this method. It was concluded that the created function yielded results with comparable accuracy and better consistency than the digitally obtained data.

A similar process was used to find a best fit curve for the turbine contours and create a function for turbine efficiency.

Compressor Component Model

Compression of the supercritical CO_2 is modeled as an adiabatic process with constant isentropic efficiency. The known inputs along with the desired outputs are shown below in Figure 9.
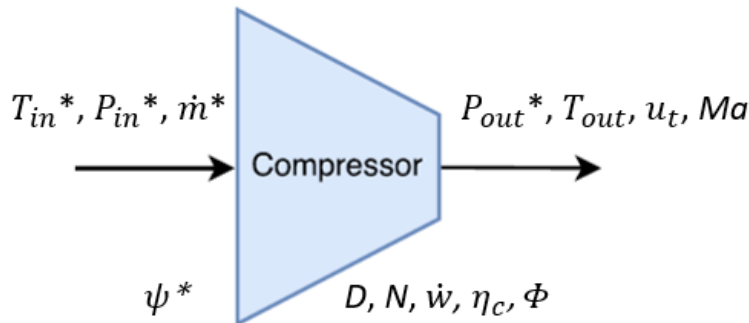

*Figure 9: Compressor model *denotes an input to the model*

A value for the head coefficient (ψ) is selected for the compressor. The head coefficient (ψ) is a

dimensionless compressor property that relates the impeller tip speed (u_t) to the isentropic enthalpy change (Δh_s).

$$\psi = \frac{\Delta h_s}{u_t^2} \tag{15}$$

The impeller tip speed is also defined by the rotor diameter (D) and the speed of the compressor shaft (ω) in radians per second.

$$u_t = \frac{D}{2}\omega \tag{16}$$

Combining Equations (9), (10), (15), and (16) a relation can be found between the head coefficient, the specific speed, and the specific diameter.

$$n_s = \frac{2}{d_s \psi^{\frac{1}{2}}} \tag{17}$$

The optimum design, or maximum efficiency compressor, will fall along the centerline of the Balje contours, as shown in Figure 5. As a result, there are two unknowns, n_s and d_s, and two equations, Equation (12) and Equation (17), which can be simultaneously solved. The compressor efficiency function previously discussed is then utilized to find the efficiency of the compressor.

If the head coefficient is set then these calculations are not repeated every time the compressor function is run. Rather, the specific speed, specific diameter, and compressor efficiency values corresponding to the head coefficient are stored for use and the compressor function utilizes them in the following calculations.

Given the inlet temperature and pressure, the inlet state of the compressor is set. As a result, the density, enthalpy, and entropy at the inlet can be found either using FIT or REFPROP.

$$\rho_{in}, h_{in}, s_{in} = F(T_{in}, P_{in})$$

The isentropic specific enthalpy at the compressor outlet is then found using the outlet pressure and the inlet entropy. This is the outlet enthalpy that would occur if the compressor was processing the fluid in an isentropic manner.

$$h_{out,s} = F(s_{in}, p_{out})$$

The isentropic compressor efficiency can also be used to find the actual enthalpy change in the compression process (Δh_a). The isentropic efficiency is defined as:

$$\eta_c = \frac{\Delta h_s}{\Delta h_a} \tag{18}$$

With the actual enthalpy change known, the work required to compress the gas can be found from:

$$\dot{w} = \dot{m}\Delta h_a \tag{19}$$

Since the outlet pressure is known, after calculating the outlet enthalpy, the outlet state is then set and the outlet temperature and speed of sound can be found with FIT or REFPROP.

$$T_{out}, a = F(h_{out,a}, p_{out})$$

The flow coefficient and the Mach number of the impeller tip are calculated as these parameters must be controlled in order to ensure a practical design. First, the volumetric flow rate is found using the mass flow rate and the inlet density.

$$\dot{V} = \frac{\dot{m}}{\rho_{in}} \tag{20}$$

With the specific speed and specific diameter known, along with the volumetric flow rate and isentropic enthalpy change, Equations (9) and (10) can be used to solve for the compressor shaft speed and the rotor diameter. The shaft speed is output to the turbine function. The diameter is used to calculate the flow coefficient, which is used to check if the solution found is realistic.

$$\Phi = \frac{\dot{m}}{\rho_{in} u_t D^2} \tag{21}$$

The Mach number of the impeller tip speed is defined as:

$$Ma = \frac{u_t}{a} \tag{22}$$

Where u_t is found using Equation (16). It is critical to maintain a low Mach number, under 1.0 to prevent shock waves, and under the threshold specified by the onset of creep fatigue.

Turbine Component Model

The expansion of the supercritical CO_2 is also modeled adiabatically assuming an isentropic efficiency. The model inputs and calculated outputs are shown in Figure 10.

$T_{in}{}^*, P_{in}{}^*, \dot{m}{}^*$ → Turbine → $P_{out}{}^*, T_{out}, Ma$

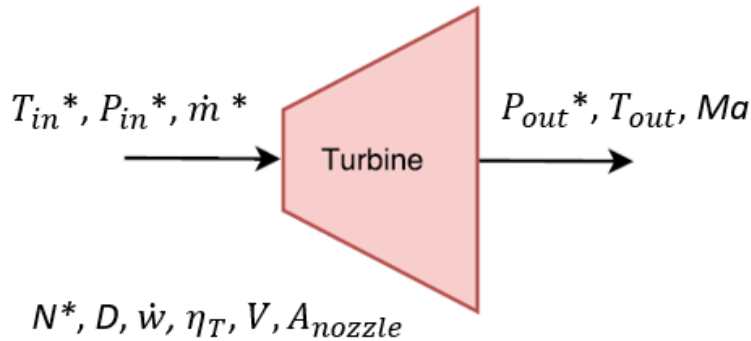$N^*, D, \dot{w}, \eta_T, V, A_{nozzle}$

Figure 10: Turbine model *denotes an input to the model

Knowing the inlet temperature and pressure, sets the inlet state of the turbine which allows the enthalpy and entropy at this stage to be calculated with FIT or REFPROP.

$$h_{in}, s_{in} = F(T_{in}, P_{in})$$

The outlet enthalpy that would occur if the turbine expanded the air isentropically can be found using the outlet pressure and inlet entropy.

$$h_{out,s} = F(s_{in}, p_{out})$$

The shaft speed for the turbine is assumed to be the same as the compressor shaft speed because they are located on the same shaft. Using the angular speed, and a guessed value for volumetric flow rate, the specific speed is found using Equation (9). Then, the maximum possible turbine efficiency for that specific speed is found using the previously discussed efficiency function.

Using this efficiency and the isentropic enthalpy change through the turbine, the turbine's power output can be calculated.

$$\dot{w} = \dot{m} \Delta h_s \eta_T \qquad (23)$$

Since the power output can also be described by the mass flow rate and the change in enthalpy, the actual outlet enthalpy can be found.

$$\dot{w} = \dot{m}(h_{in} - h_{out}) \qquad (24)$$

Knowing the outlet pressure and enthalpy, the other outlet conditions, temperature, speed of sound, and density, can be found using FIT or REFPROP.

$$T_{out}, a, \rho_{out} = F(h_{out,a}, p_{out})$$

Then the resulting volumetric flow rate is found using the mass flow rate, the outlet density, and Equation (20). There is an error value between the guessed volumetric flow rate and the resulting volumetric flow rate. The MATLAB fzero routine is used to bring this error value to zero and find the correct volumetric flow rate. The spouting velocity (C_s), which would occur if the supercritical CO_2 expanded isentropically through the turbine, can be found using the isentropic enthalpy change.

$$C_s = \sqrt{2\Delta h_s} \qquad (25)$$

The effective nozzle area can be found using the spouting velocity, the mass flow rate, and the outlet fluid density.

$$\dot{m} = C_s A_{nozzle} \rho_{out} \qquad (26)$$

The diameter of the turbine is found using the specific diameter previously calculated from the specific speed and Equation (10). Using the diameter and the shaft speed, the tip velocity of the turbine can be found.

$$u_t = \frac{D}{2} N \qquad (27)$$

The ratio of tip velocity to spouting velocity (V) can be solved for to check if the solution found is realistic.

$$V = \frac{u_t}{C_s} \qquad (28)$$

It is also important to be sure the Mach number at the outlet remains subsonic to prevent shock waves in the turbine and low enough to prevent creep fatigue. Therefore, the Mach number is calculated with the tip speed and the outlet speed of sound.

$$Ma = \frac{u_t}{a} \tag{29}$$

Radiator Component Model

As an initial approximation, the heat rejection system was modeled as a simple radiator, as shown in Figure 11. However, the actual radiator in this system will likely have a secondary loop integrated with the supercritical CO_2 loop.
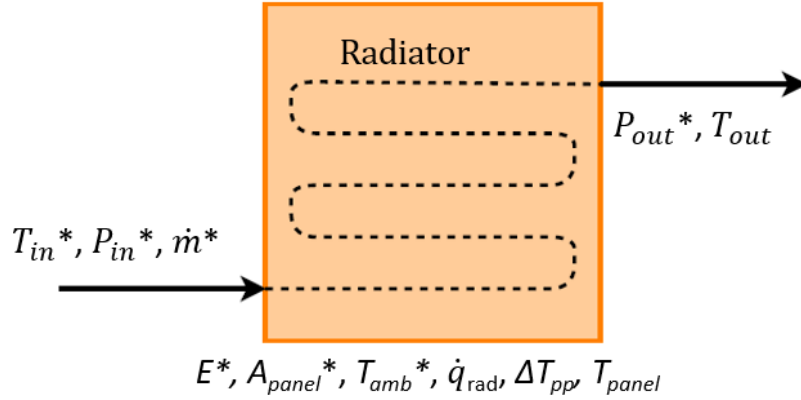

*Figure 11: Radiator model *denotes an input to the model*

The inlet enthalpy was found as a function of the inlet temperature and pressure. Then, to calculate the properties of the supercritical CO_2 after passing through the radiator, an iterative process was utilized. A value was guessed for the outlet enthalpy. This guessed value was then used to calculate the heat transfer from the fluid to the radiator.

$$\dot{q}_{rad} = \dot{m}(h_{in} - h_{out}) \tag{30}$$

At steady state operation, the heat transfer from the radiator to the environment is equivalent to the heat transfer from the fluid to the radiator. Therefore, the radiative heat transfer equation is then used to find the temperature of the panel at steady state. Here, the emissivity was assumed to be 0.9.

$$\dot{q}_{rad} = A_{panel}\varepsilon\sigma(T_{panel}^{\;4} - T_{amb}^{\;4}) \tag{31}$$

It is known that the outlet temperature of the radiator is slightly larger than the steady state panel temperature. This difference is defined as the pinch point temperature change (ΔT_{pp}).

$$T_{out} = T_{panel} + \Delta T_{pp} \tag{32}$$

The final outlet enthalpy is then found as a function of the outlet pressure and the calculated outlet temperature.

$$h_{out} = h(T_{out}, P_{out}) \tag{33}$$

This calculated outlet enthalpy is then compared to the guessed outlet enthalpy. Various values were selected as guesses for the outlet enthalpy between zero and the inlet enthalpy. The corresponding

error values were evaluated to find a range containing the enthalpy value with zero error. Then the MATLAB fzero function is again used to find the correct outlet enthalpy value.

Cycle Modeling

The component models were integrated to create a simple, recuperated Brayton cycle, as shown in Figure 1.The cycle model takes the mass flow rate ($\dot{m}$), the low side pressure (p_1), the highest temperature in the cycle (T_4), the compression ratio of the compressor (PR_c), the conductance of the recuperator (UA), the panel area of the radiator (A_{panel}), the ambient temperature (T_{amb}), the type of fluid, and whether the desired method for property finding is FIT or REFPROP.

In this function, the first step is to find the pressures at every state. The user supplied pressure ratio of the compressor is used to find the outlet pressure of the compressor.

$$PR_c = \frac{p_2}{p_1}$$

(34)

The pressures at states 3, 4, 5, and 6 were found using values for expected or allowable pressure drop in the recuperator, reactor, and radiator. Typical values for these pressure drops are 0.52% for the cold side of the recuperator, 1.5% for the hot side of the recuperator, 2.7% for the reactor, and 1% for the radiator [6].

To find the desired cycle parameters, a temperature for the compressor inlet is guessed. The guessed value is constrained between the lowest supported temperature in FIT (240 K) and the user supplied turbine inlet temperature, T_4. The guessed temperature sets state 1, and the compressor model can be used to find the temperature at state 2. Since the temperature at state 4 is a user input, and the pressure has already been solved for, state 4 is also set. The turbine model is then used to find the temperature at state 5 and set that state as well. Since states 2 and 5, the cold and hot recuperator inlets respectively, are set, the recuperator model can then be used to set states 3 and 6. The radiator model is then used to get from state 6 to state 1, giving a new value for the initially guessed T_1. As expected, there will be some error between the initial guessed value for T_1 and the final calculated value. As done previously, the MATLAB fzero routine is used to find the value for T_1 where the error value is zero.

Since states 3 and 4, before and after the reactor respectively, are set, the heat required from the reactor can be found.

$$Q_{reactor} = \dot{m}(h_4 - h_3)$$

(35)

The cycle power output is found to allow for easy cycle comparison.

$$\dot{W}_{net} = \dot{W}_t - \dot{W}_c$$

(36)

With the power output and the heat input, the efficiency of the cycle is calculated as:

$$\eta_{cycle} = \frac{\dot{W}_{total}}{Q_{reactor}}$$

(37)

Preliminary Optimization

The first optimization step is to find the lowest mass recuperator which can give the desired power

output of 40 kW for a given set of input parameters. For any recuperator conductance, as the mass flow rate increases, the cycle's power output also increases until it reaches a peak value. Then, the cycle's power output begins to decrease because the recuperator effectiveness begins to drop dramatically. The curves for several conductances ranging from 1 kW/K to 10 kW/K are shown in Figure 12.
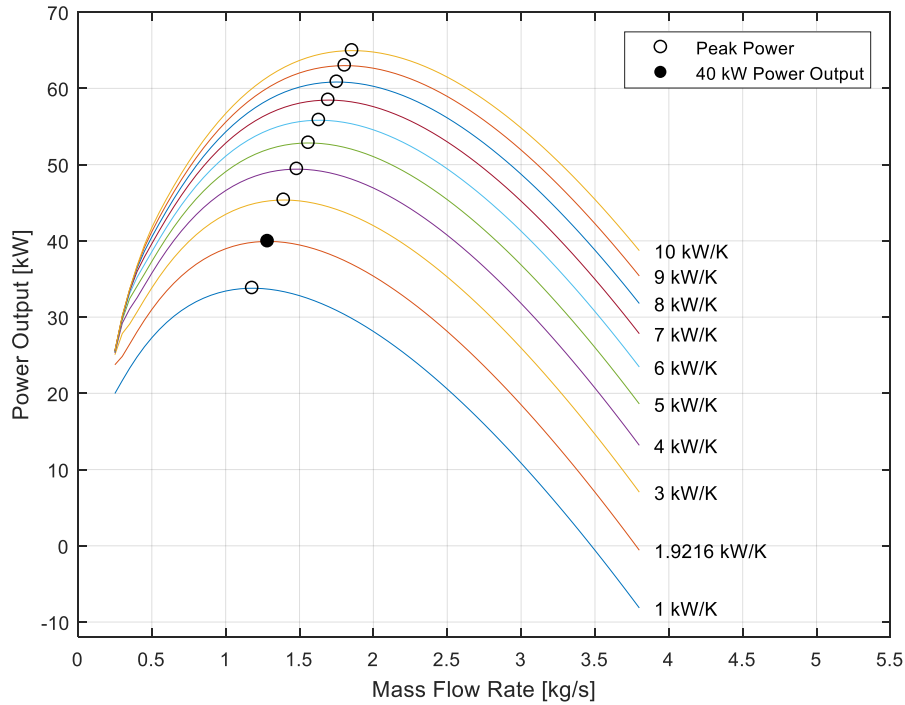

Figure 12: Power output vs. mass flow rate for several conductances with cycle parameters p_1=9,000 kPa, T_4=1,100 K, PR_c=2, T_{amb}=100 K, and A_{panel}=100 m^2, supercritical CO_2 as the fluid, and FIT as the property database

The closed point in Figure 12 represents the cycle with the lowest possible recuperator mass which can produce 40 kW of output power. To find this conductance, a conductance value is guessed, and the quadratic approximation method is used to find the maximum achievable output power for that conductance. Then an error value is calculated between that maximum power and the desired cycle power. The guessed conductance value is initially chosen by testing a few set conductances and selecting the one with the lowest error value. Then the MATLAB fzero function is used to find a conductance where the error value between the maximum power output and the desired power is zero.

The conductantance found is used as a minimum bound. Moving along the 40 kW line, to the left of the closed point, there are several other possible cycle formations. These cycle formations have a higher conductance, signifying a larger recuperator, but they also have a higher cycle efficiency meaning a smaller amount of heat output is required from the reactor. The reactor heat output required for a power output value of 40 kW was found for recuperator conductances between 2 kW/K and 25 kW/K. The relationship between recuperator size and required reactor heat output can be seen in Figure 13.
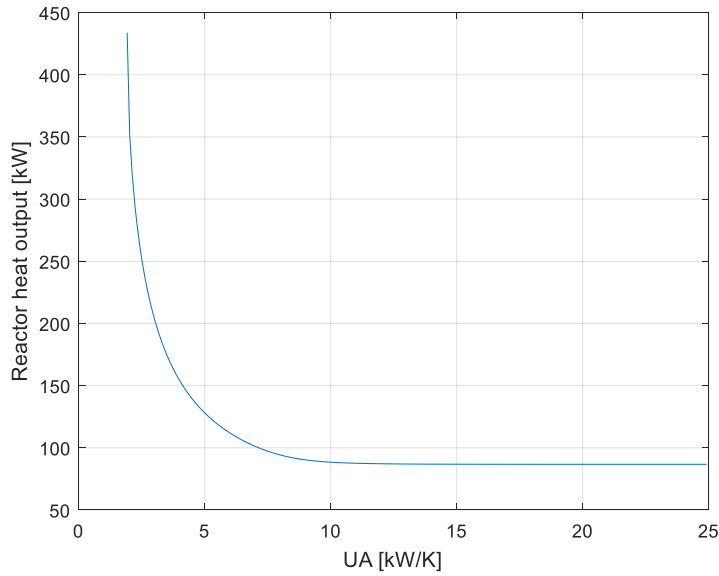
Figure 13: Required reactor heat output as a function of recuperator conductance for cycle parameters p$_1$=9,000 kPa, T$_4$=1,100 K, PR$_c$=2, T$_{amb}$=100 K, and A$_{panel}$=100 m^2, supercritical CO$_2$ as the fluid FIT as the property database, and 40 kW of output power

Figure 13 shows that as the recuperator conductance becomes small the size of the reactor asymptotically increases, and as the size of the reactor becomes small the size of the recuperator asymptotically increases. In either of these too limits, the mass of the system becomes very large; therefore, It is hypothesized that there will be a cycle formation between the two extremes which minimizes the sum of the two masses.

The reason behind the increased efficiency for larger recuperator conductances is the position of the compressor stage of the power cycle in a TS diagram as seen in Figure 14.
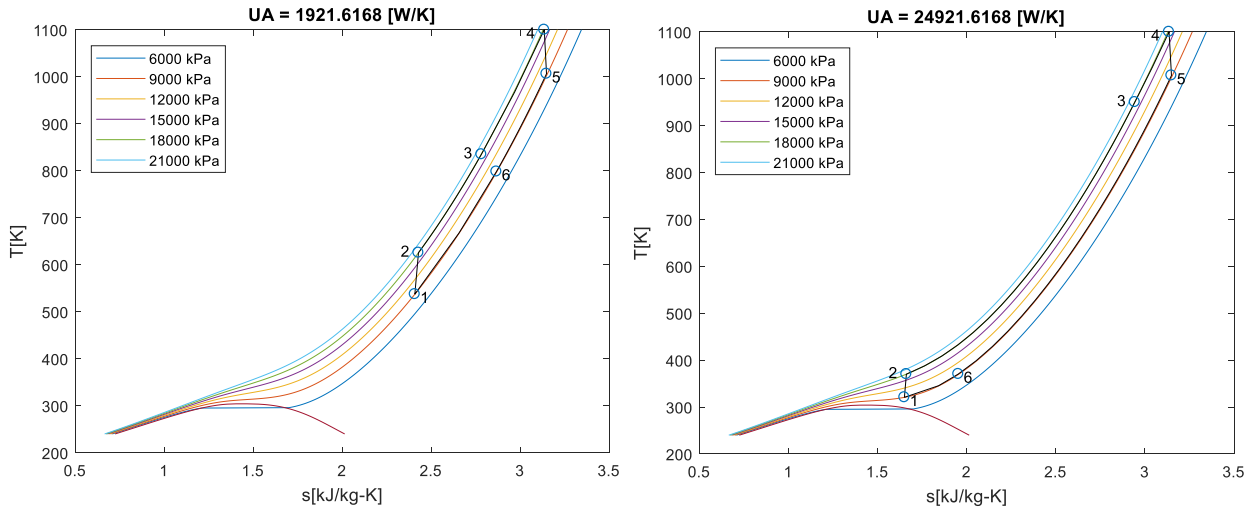

Figure 14: Comparison between TS diagrams for large and small recuperator conductances for cycle parameters p$_1$=9,000 kPa, T$_4$=1,100 K, PR$_c$=2, T$_{amb}$=100 K, and A$_{panel}$=100 m^2, supercritical CO$_2$ as the fluid FIT as the property database, and 40 kW of output power

Figure 14 shows that with higher conductances, the cycle is very near the vapor dome for the compressor stage. At this state, the CO_2 has a very high density, allowing for very high compressor efficiency, and therefore very high cycle efficiency.

To find the mass optimum cycle, mass correlations are needed for parameters corresponding to the size of the recuperator, reactor, and radiator. Using an existing microtube shell and tube heat exchanger as an example, it is possible to approximately relate the recuperator's conductance and mass according to [7]:

$$m_{recuperator} = 0.0131 \left[\frac{\text{kg K}}{\text{W}} \right] (UA)$$

(38)

Once an acceptable model for the reactor mass is created, a cycle with optimum mass will be apparent for any specific radiator panel area. Using an example of an existing radiator system with capillary pumped loops and a conical thermal radiator, the relation between that radiator panel area and the radiator's mass is found as [8]:

$$m_{radiator} = 5.8684 \left[\frac{\text{kg}}{\text{m}^2} \right] (A_{panel})$$

(39)

Then, sweeping through panel areas will give an overall mass optimized simple, recuperated Brayton cycle.

REACTOR INFORMATION

Since standard reactor modeling approaches are too computationally expensive for integration in a system optimization algorithm, a surrogate reactor model is being created that can be incorporated into the power cycle model to allow a complete and comprehensive optimization of the power system. Given a set of power cycle flow conditions, the model will minimize the total reactor mass. The reactor mass is dependent on fuel type, fuel enrichment, and reactor geometry. The reactor model will fit into the system optimization to iterate with the power cycle, in order to minimize overall system mass.
Some initial design choices were made to guide the reactor model development. Since reactor fuel choice has a significant impact on design parameters, it was important to pick a fuel before iterating through different geometric configurations. The following targets were desired in a reactor fuel choice.

1. Large volumetric power density
2. High melting temperature
3. 10 year lifetime without refueling

A large thermal power density reduces the overall fuel mass required to produce a given thermal power. It also shrinks the overall size of the reactor, reducing the pressure vessel thickness requirements. The achievable power density is limited, in part, by the melting temperature of the fuel, so higher melting temperatures enable higher power densities. A higher melting point also allows higher coolant temperatures, thus increasing power cycle efficiency and reducing the required thermal reactor power.

Traditional ceramic reactor fuels (pin and clad) do not meet the power density and temperature requirements necessary for the design goals. Advanced fuel concepts, such as ceramic-metallic CERMET fuel, have been studied by NASA for use in nuclear rockets [9]. CERMET fuel contains suspended uranium fuel particles in a metal matrix. The metallic matrix strengthens the fuel, limiting swelling and

fission product release. It also provides pathways of high thermal conductivity. These pathways allow large volumetric power density compared to traditional fuel and they also help flatten temperature profiles in the fuel, which limits fuel swelling. The design will use CERMET fuel with highly-enriched UN fuel in a tungsten matrix. The fuel will be hexagon-shaped with coolant flow channels through the middle of each hexagonal fuel element. Using highly-enriched uranium (>20% 235U) allows the design to meet the target lifetime and power level with less overall fuel mass.

Traditionally, nuclear reactor design often treats the reactor separately from the power cycle. A power cycle is chosen and a reactor is designed to drive the cycle. There may be some iterations between the designs but they are largely developed independently of each other. For a comprehensive system mass optimization, this separate treatment is no longer viable. The mass of the power cycle and reactor are intrinsically coupled via the thermodynamic efficiency of the power cycle, flow conditions, and the desired electrical output of the system. Therefore, to perform an overall system mass optimization, the reactor design and power cycle parameters must be updated consistently during iterations to identify the minimum system mass.

Existing reactor physics software used to design nuclear reactors is computationally intense. It would be prohibitively expensive to invoke these software packages during each iteration of the system optimization. To this end, a surrogate model is being developed to calculate a minimum reactor mass of a valid reactor design, within certain constraints, as a function of flow conditions, cycle efficiency, reactor fuel, and desired electrical output. There are two important types of analysis to consider for design validity. The first is coolability; the generated heat must be removed from the core without material damage. The second consideration is neutronics; the reactor must remain critical at the desired power level, for the lifetime of the power system. The main source of mass in a nuclear reactor is the fuel and the pressure vessel. The pressure vessel and fuel mass are both proportional to the volume of fuel. The lowest volume design minimizes total reactor mass.

The first step in the surrogate modeling process will be to identify coolable designs; the reactor must operate at full power without compromising the integrity of the fuel. The minimally cooled designs maximize fuel power density to minimize required fuel mass. Given power cycle requirements (coolant mass flow, dT, core inlet state conditions), a parametric sweep of reactor geometric parameters will be performed. For a fixed reactor length, the sweep will identify a single coolable design for various combinations of fuel channel radii and fuel thicknesses. The result of each design will be a number of fuel channels that match the required thermal input for the power cycle.

The next step will be to ensure the neutronics viability of the design. The reactor must be large enough to sustain a fission chain reaction throughout its target lifetime. Every combination of coolant channel radius and fuel element pitch will result in a reactor configuration that satisfies the needs of the power cycle. Each of those configurations will be subject to a neutronics analysis to determine if that configuration will meet reactor physic requirements, and if not, how much larger it must be. In particular, adding fuel channels may be required to operate the reactor at full power for the desired ten-year life span. From each design result, the reactor mass will be calculated.

The thermal-hydraulics and neutronics analysis will be used to find the minimum sized reactor for a variety of power cycle conditions, selected throughout the domain of the power cycle design. These data points can then be used for a surrogate model that can rapidly approximate the minimum-sized

reactor for any points in that domain. This model can then be integrated within a global system optimization to seek the minimum total system mass including both the reactor and other components.

CONCLUSION

A robust recuperated Brayton cycle model has been created and is being utilized in the design of an optimization model. Research of existing recuperators and radiators have provided an approximate mass correlation against conductance and panel area for the two components respectively. A highly mass efficient nuclear reactor model is being developed simultaneously to provide the correlation between the mass of the reactor and the necessary heat output with the existing flow parameters.

The next steps of this project will include integrating the cycle optimization model with the nuclear reactor model to incorporate the mass of the reactor. After this is done, the tradeoffs between the sizes of the three components will be observed, and a mass optimum cycle will be apparent.

The optimization will be also tested with various cycle parameters, pressures, pressure ratios, and temperatures. Other cycle configurations, such as recompression and intercooling, will be investigated along with other options for working fluid. Another potential project addition is a more robust and accurate radiator model, taking into account the mass cost of a secondary loop.

ACKNOWLEDGEMENTS

REFERENCES

[1] E. W. Lemon, M. L. Huber and M. O. McLinden, *NIST Standard Reference Database 23: Reference Fluid Thermodynamic and Transport Properties-REFPROP, Version 9.1, National Institute of Standards and Technology,* Gaithersburg, 2013.

[2] J. Dyreby, *Fluid Interpolation Tables-FIT, Northalnd Numerics LLC,* Madison, 2016.

[3] G. Nellis and S. Klein, Heat Transfer, New York: Cambridge University Press, 2009.

[4] J. J. Dyreby, *Modeling the Supercritical Carbon Dioxide Brayton Cycle with Recompression,* Madison: University of Wisconsin-Madison, 2014.

[5] O. E. Balje, Turbomachines, New York: John Wiley & Sons, 1981.

[6] M. J. Barrett and P. K. Johnson, "Performance and Mass Modeling Subtleties in Closed-Brayton_Cycle Space Power Systems," 2005.

[7] Y. Jiang, E. Liese, S. E. Zitney and D. Bhattacharyya, *Optimal Design of Microtube Recuperators for an Indirect Supercritical Carbon Dioxide Recompression Closed Brayton Cycle.*

[8] R. J. Lipinski, S. A. Wright, M. P. Sherman, R. X. Lenard, A. C. T. R. A. Marshall, D. I. Poston, R. Kapernick, R. Guffee, R. Ried, J. Elson and J. Lee, *Small Fission Power Systems for NEP,* American Institute of Physics, 2002.

[9] R. Hickman, B. Panda and S. Shah, "Fabrication of high temperature CERMET materials for nuclear thermal propulsion," 2005.